AIAA JOURNAL
Vol. 30, No. 7, July 1992

Characterization of Damping of Materials and Structures from Nanostrain Levels to One Thousand Microstrain

J. M. Ting*
Advanced Composites Laboratories, Waltham, Massachusetts 02154
and
E. F. Crawley†
Massachusetts Institute of Technology, Cambridge, Massachusetts 02139

Results are presented from an experimental study performed to characterize material and structural damping over a range of strain from 1 nanostrain (nε) to 1000 microstrain ($\mu\varepsilon$). Material damping was measured in aluminum rectangular bars and tubes and laminated graphite/epoxy bars and tubes. Structural damping was measured in a precision, three-dimensional tetrahedral truss consisting of ball nodes and tubular bars. Damping ratios were obtained via a sine sweep approach using piezoceramic strain sensors and piezoceramic proof mass actuators. Results showed that material damping is generally independent of strain below 10 $\mu\varepsilon$. Experimental damping measured at small strain levels compared well with theoretical models where available. Material damping showed a dependence on a strain at levels above 100 $\mu\varepsilon$ and could be modeled for metals by the movement of dislocations. Structural damping was independent of strain below at least 10 $\mu\varepsilon$.

Introduction

RECENTLY, an effort has been made to develop large, space-based astronomical instruments such as the Hubble Space Telescope (HST) and its possible successor, a space-based optical interferometer.[1] The optical elements of these and other future optical instruments must be held stable relative to each other within fractions of a wavelength of light.[2] To achieve the rigorous requirements for alignment and positioning, there is a need for passive damping, perhaps supplemented by active control. In either a passive or active design, a knowledge of passive damping establishes limits on the achievable performance. The operating wavelength and precision requirements of these instruments implies that the strain amplitudes at which this damping is important is on the order of nanostrain to microstrain (i.e., 10^{-9}–10^{-6})—orders of magnitude smaller than the amplitude at which structural dynamic characterization commonly occurs.

Previously, there was uncertainty in the aerospace community about the damping of structures at such small amplitudes.[3] One school of thought argued that structures will behave linearly by design and the properties will be constant with strain level. The other school of thought argued that the mechanisms that normally provide structural damping, atomic and thermal diffusion, plane slippage, joint friction, and so forth, will no longer function at very small strains. This uncertainty led to an effort to study the behavior of structures at nanostrain levels of motion.

The objective of the research presented was to characterize the damping of materials and structures from nanostrain (nε) levels to 1000 microstrain ($\mu\varepsilon$), that is, a millistrain (mε). To do this, specimens of typical spacecraft materials, aluminum and graphite/epoxy, in typical space structural member cross sections were tested. To study pure material damping in a simple geometry, rectangular cross section bars were constructed of aluminum and graphite epoxy. To study material damping in a slightly more complex form, tubes of aluminum and graphite/epoxy were also constructed. The material damping specimens were fabricated with various lengths to permit the study of damping over a range of frequencies. Structural damping in a built-up structure was determined by testing a tetrahedral space truss. The truss, part of a testbed in the Space Engineering Research Center (SERC), was designed to be prototypical of the structure of a space-based optical interferometric telescope. Three and one-half meters on a side, the six-arm tetrahedral truss was constructed from aluminum ball nodes and aluminum tubes connected with tight joints. The material and structural damping specimens were tested for values of critical damping ratio using a sine sweep or resonant flexural approach over a range of strain from 1 nε to 1000 $\mu\varepsilon$ to find if there was any dependence of damping on strain level. This range of specimens encompasses many passive loss mechanisms inherent in structures: thermoelastic, dislocation motion, viscoelastic, and joint friction. Because these same loss mechanisms underlie many passive damping augmentation schemes, the measured trends of damping vs strain level also can be extended to these damping enhancement schemes.

Normally, experimental measurement of damping is done at moderate strain levels. The range from 10 to 1000 $\mu\varepsilon$, is typical of structural dynamic testing. Previous work done at these strain levels include that of Zener,[4] Ke,[4] Granick and Stern,[5] and Mohr,[6] who measured internal damping in metals, and Lesieutre,[7] van Schoor,[8] Gibson and Plunkett,[9] and Bert,[10] who made additional measurements of damping in composite laminates. Testing from 1 nε to 1000 $\mu\varepsilon$ would, therefore, encompass the actual operating range of the instruments and the range in which measurements are traditionally taken. To characterize damping at nanostrain levels, the additional challenge of measuring nanostrain vibrations had to be addressed. Techniques for doing this had previously been developed in the field of gravity wave detection.[11,12] The approach developed using piezoceramic strain sensors, was adapted for use in this study.

In this article, a discussion of the development of the sensors and measurement techniques is presented. As a result of

Presented as Paper 91-1125 at the AIAA/ASME/ASCE/AHS/ASC 32nd Structures, Structural Dynamics, and Materials Conference, Baltimore, MD, April 8–10, 1991; received April 22, 1991; revision received Nov. 6, 1991; accepted for publication Nov. 19, 1991.

*Engineer; former Graduate Research Assistant, Massachusetts Institute of Technology. Member AIAA.

†Professor of Aeronautics and Astronautics, Space Engineering Research Center. Associate Fellow AIAA.

the development of these techniques, measurements of modal critical damping ratio ζ could be made down to peak strain levels of 1 nε. Results from the tests of the aluminum bars over a range of frequencies from 6 to 174 Hz, the aluminum tubes over a frequency range from 183 to 830 Hz, the graphite/epoxy bars over a frequency range from 30 to 150 Hz, the graphite/epoxy tubes over a frequency range from 275 to 500 Hz, and the structural damping test specimen over a frequency range form 40 to 55 Hz are presented and discussed. The measured damping ratios due to material damping are compared with results from models of the material damping where available. The damping in specimens constructed from aluminum is compared with the model based on the thermoelastic relaxation of solids developed by Zener,[4] and the model of damping incorporating motion of dislocations developed by Boser.[13] Damping in specimens constructed from graphite/epoxy is compared to results obtained using models developed by Adams and Bacon,[14] and Ni and Adams.[15]

Test Instrumentation and Procedure

Due to the low strain levels at which measurements were made and the inherent low damping and light mass of the specimens, a sensitive, precise, nonobtrusive technique was developed to excite the specimens, measure their response, and characterize their damping. To sense and actuate vibrations in the material and structural damping test specimens, the specimens were instrumented with piezoceramic strain sensors and excited with piezoceramic proof mass actuators. These sensors and actuators were chosen because they were found to best meet the requirements defined by the objectives of the experiment: to actuate strains and provide measurements from which strains could be inferred down to 1 nε with good signal to noise content. Other instrumentation approaches that were evaluated but discarded included conventional foil and semiconductor strain gages (not sufficiently sensitive), laser velocimetry (not sufficiently sensitive), optical interferometry (the need for bulky mirrors), and accelerometers (not sufficiently sensitive). In this section, the method selected for instrumenting the test specimens is discussed as well as the procedure used to test them.

The strain sensors were small rectangular wafers manufactured from 0.25-mm-thick sheets of a G-1195 piezoceramic material.[16] Two different size sensors were applied to the test specimens of the two different geometries. The sensors used on the flat rectangular bar specimens were 6.4 mm wide by 12.7 mm long and were bonded directly to the surfaces of the bars using a cyanoacrylate adhesive. The sensors used on the tube specimens, as shown in Fig. 1, and on the single, instrumented strut of the testbed were 3.2 mm wide by 12.7 mm long. These sensors were bonded to small flat areas milled into the surfaces of the tubes.

All piezoceramic sensors were calibrated in situ against resistive foil strain gages operating in the effective range of the foil strain gauges (0.1–100 $\mu\varepsilon$). The response of piezoceramic sensors has been shown to be linear down to at least 10 pε.[12] On each flat, rectangular bar specimen, a single strain gage was placed next to the side of the piezoceramic sensor. As shown in Fig. 1, on each of the tube specimens and the testbed strut, two strain gages were placed on either end of the piezoceramic sensors. For all the test specimens, the strain sensors were placed such as to allow the sensing of several mode shapes. Because the specimens were tested in flexure, the strain fields throughout the specimens were nonhomogeneous along the length of the specimen and through the thickness. The measured surface strains were adjusted using the spatial mode shapes to obtain values of strain that were maximum throughout the specimen. The calculated data reported are these maximum strains. Because the reported damping is the damping of the entire specimen while the reported strain is a single value in a distributed field, care must be used in interpreting the plots of damping vs strain. It is safe to say, though, that the regions in which damping is constant truly show regions in which the damping is independent of maximum strain.

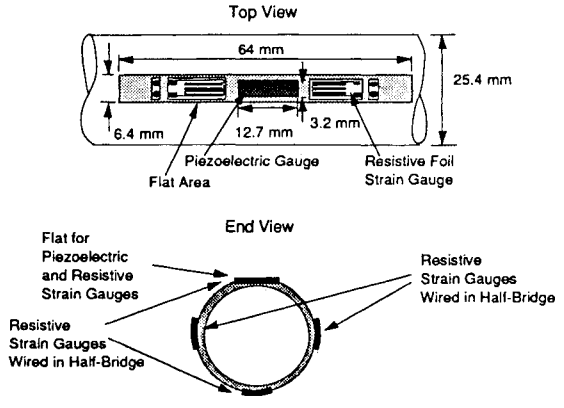

Fig. 1 Instrumentation of tube specimens with sensors.

The specimens were actuated with piezoceramic proof mass actuators. The actuators, 12.7 mm × 38 mm × 0.53 mm rectangular plates, were cut from sheets of G-1195 piezoceramic material in a bimorph form. In a bimorph form, two oppositely polarized sheets of the 0.25-mm-thick material are bonded to either side of a 0.03-mm-thick sheet of metallic shim, so when a voltage is applied across the device, the opposing strains cause the device to bend. The bending motors were cantilevered from the tips of the material damping test specimens to actuate the specimens in flexture. On the bar specimens, the actuators were bonded directly to the ends of the specimens, that is, in areas of low strain. On the tube specimens, the actuators were bonded to small, raised flats machined from aluminum that were bonded to the ends of the tubes. On the testbed, an actuator was bonded to the end of a platform made of a small piece of aluminum bolted to a node. To excite strains above 10 $\mu\varepsilon$ in the material damping test specimens, small weights were added to the tips of the actuators to increase the proof mass. For large strain tests of the structural damping test specimen, the interferometer truss, a dc motor proof mass actuator was used.

After instrumenting the material and structural damping specimens, tests were performed to obtain values of critical damping ratio. First, the material damping test specimens were suspended using wires and soft springs at the nodes of their free-free mode shapes. The structural damping test specimen were suspended using wires and soft springs at the vertices of the tetrahedral truss. Then, damping was measured using a sine sweep procedure. A Phillips PM-5191 programmable synthesizer/function generator was used to drive the actuators. This device was capable of holding a prescribed frequency down to 0.1 mHz. While keeping the force constant, the output strain was measured with a high precision, two-phase lock-in amplifier, model 5210 manufactured by PAR. Values of critical damping ratio were obtained using

$$\zeta = \frac{\Delta\omega}{2\omega_n}$$

where ω_n was the natural frequency of the mode of vibration, and $\Delta\omega$ was the frequency difference between the two half-power points. Because the force was kept constant, the output strain was proportional to the transfer function and varied during each sweep. The reported strains are the maximum strains during each sweep. At least six sweeps were performed to obtain values of ζ at each peak output strain level, which were averaged to give the average damping ratio reported.

The sources of imprecision in the experiment were the resolution of the digitally controlled frequency generator and the signal noise, the latter dominant. To reduce the effects of

electrical and mechanical noise on the material damping measurements, tests for material damping were performed in a metal vacuum chamber, 4.27 m high and 3.05 m in diameter that acted as a Faraday cage and acoustic isolator. To reduce mechanical noise, specimens were suspended using two soft spring suspension systems, each consisting of three springs and three lead masses. The frequency of the highest mode of the system was 0.9 Hz with a mechanical isolation of 40 dB at the lowest specimen frequency tested, 6 Hz. The precision of the damping measurements, which corresponds to the resulting noise level, was calculated for each test point and is shown as a bar in the data figures, of which Fig. 2 is an example. For strain levels near 1 nε, the imprecision due to noise is large, but diminishes rapidly at higher strains. For most test cases, the precision limit from the noise is less than $\pm 0.01 \times 10^{-3}$ in ζ. To further bound the precision, the minimum, maximum, and average of the six or more sine sweeps are shown on the data figures. The difference between the minimum and maximum was generally less than 0.04×10 ζ. From this it can be inferred that the precision of the experiment was on the order of $\pm 0.02 \times 10^{-3}$ in ζ. The sources of inaccuracy were air drag and transmission losses through the suspension. To reduce the effects of air, measurements of material damping at large strain levels, from 10 to 1000 $\mu\varepsilon$, were performed in a vacuum of 10^{-2} Torr. Measurements at small strain levels, from 1 nε to 10 $\mu\varepsilon$, were performed in air and corrected using two models of aerodynamic damping.[17] One model was based on the friction in a viscous boundary layer around the oscillating specimens that was independent of amplitude and another model was based on the damping due to quasisteady drag that was dependent on amplitude.[17] Results from tests performed in vacuum and air showed that the model based on viscous effects was the more applicable model up to the maximum strain levels reached in this study. When not taken in vacuum, the results in the data figures of material damping are corrected for air using results from both models with the unsteady viscous model dominating. These corrections are on the order of 0.1×10^{-3} to 0.01×10^{-3} in ζ for the material damping results.

Because of limitations of size and instrumentation, tests of the truss were performed in air. Predictions of the air damping effects on the truss were made using the same formulation as that used and verified for the material damping specimens. The effect on each strut and node was modeled individually and then summed over the entire structure. The quasistatic drag model was found to have a greater effect at large strain levels than the unsteady viscous model. Air damping corrections for the structural damping measurements were an order of magnitude higher than those for the material damping measurements, from 1.0×10^{-3} to 0.1×10^{-3}.

Transmission losses of both the material and structural damping specimens were minimized by suspending the test specimens at their nodes and were estimated to be 0.2×10^{-3} in ζ. Thus, the experiment to measure material damping is expected to have an accuracy of 0.2×10^{-3} and a precision of 0.02×10^{-3} in ζ, while the experiment to measure structural damping is expected to have an accuracy ranging between 0.2×10^{-3} to 1.0×10^{-3} and a precision of 0.02×10^{-3} in ζ.

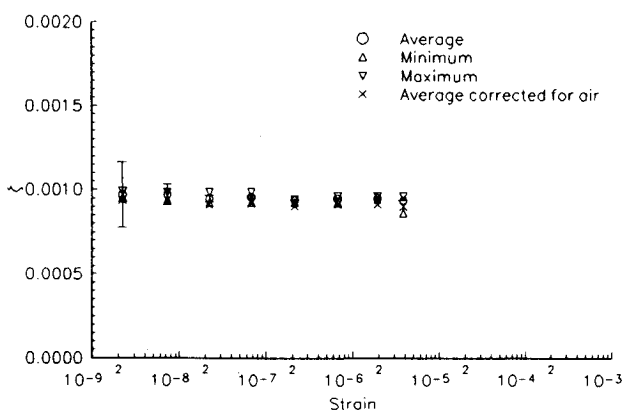

Fig. 2 Damping in second mode of 1.3-m aluminum bar in air, f = 25.8 Hz.

Material Damping Test Results

Aluminum

The first tests were conducted on bars and tubes of aluminum to find the pure material damping in a specimen with a simple geometry made of a common aerospace material that has a well-documented and predictable level of damping. Rectangular bars of 6061-T6 aluminum were constructed with a cross section 26 mm wide and 3.2 mm thick. As postulated by Zener,[4] the nonhomogeneous strain field in a metallic bar tested in flexure causes thermal gradients and heat flow. The rate of heat flow is determined by the thermal properties of the material. The mechanical, cyclic frequency can be matched to the relaxation frequency ω_r, which is related to the amount of time needed for heat to flow from one face to the other. This frequency is given by

$$\omega_r = \frac{h^2 C \rho}{\pi^2 k} \tag{2}$$

here h is the thickness of the specimen, C is the specific heat per unit mass, ρ the material density, and k the thermal conductivity.[4] For the material properties and dimensions of the aluminum specimens, ω_r = 9.91 Hz.[19] As listed in Table 1, the bars were manufactured with lengths of 0.5 m, 0.9 m, 1.3 m, and 1.7 m to give a wide range of test frequencies that bracket the Zener relaxation frequency.

To obtain values of material damping of the same material in a more typical geometry, tubes were fabricated of 6061-T6 aluminum with a 26-mm outer diameter and a 1.7-mm wall thickness. These dimensions were chosen to give the same width and total wall thickness as the bars. The tube specimens were cut from the same piece of tubing stock into 0.9-m and 0.7-m lengths as listed in Table 1.

A total of seven flexural modes of the rectangular bars were tested over the lower strain range in air from 1 nε to 10 $\mu\varepsilon$. The results from these tests are summarized in Table 1. Included in the table are the length and type of each specimen, the frequency of the mode tested, the range of strain over which the damping was found to be independent of strain, the average damping ratio, the average damping ratio corrected for air effects, and the damping ratio predicted by the Zener model for the bars at room temperature. Also, given in Fig. 2 is a plot of damping ratio obtained over the small strain range in air as a function of strain for the second mode of the 1.3-m aluminum bar at 25.8 Hz. As indicated in Table 1 and shown in Fig. 2, the damping shows little variation with strain amplitude below 10 $\mu\varepsilon$, within the bounds of the precision and accuracy of the measurements.

The results from the aluminum bars at small strains can be compred with predictions from the Zener model based on the thermoelastic relaxation.[4] Although thermoelastic relaxation is but one of many damping mechanisms, the Zener model has been shown to correlate well with experimental results, giving a lower bound on damping.[8] Those predictions are listed in Table 1 and are also plotted against frequency, nondimensionalized using the theoretical relaxation frequency, with the experimental results in Fig. 3. As shown in Fig. 3, the experimental results show good correlation with the theoretical results. The measured data are consistently 0.1–0.2 $\times 10^{-3}$ in ζ above the predicted result, which is consistent with the expected accuracy of the experimental procedure.

Table 1 Material damping test results for aluminum specimens

Type	Length, m	Frequencies tested, Hz	Strain independent range	Average damping ratio	Corrected damping ratio	Predicted damping ratio
Al/bar	1.7	6.17	1.42 nε– 0.968 με	1.24×10^{-3}	1.17×10^{-3}	0.98×10^{-3}
		17.1	1.18 nε– 1.62 με	1.27×10^{-3}	1.23×10^{-3}	0.95×10^{-3}
Al/bar	1.3	9.35	1.30 nε–78.1 με	1.36×10^{-3}	1.30×10^{-3}	1.09×10^{-3}
		25.8	2.22 nε– 3.82 με			
		50.6	2.02 nε–12.4 με	0.59×10^{-3}	0.56×10^{-3}	0.41×10^{-3}
Al/bar	0.9	19.5	92.6 nε– 5.88 με	1.16×10^{-3}	1.12×10^{-3}	0.89×10^{-3}
Al/bar	0.5	173.6	8.25 nε–13.3 με	0.26×10^{-3}	0.25×10^{-3}	0.12×10^{-3}
Al/tube	0.9	185.2	10.8 nε–78.9 με	0.07×10^{-3}	0.06×10^{-3}	—
		510.3	1.10 με–11.1 με	0.12×10^{-3}	0.12×10^{-3}	—
Al/tube	0.7	308.1	20.9 nε–19.6 με	0.12×10^{-3}	0.11×10^{-3}	—

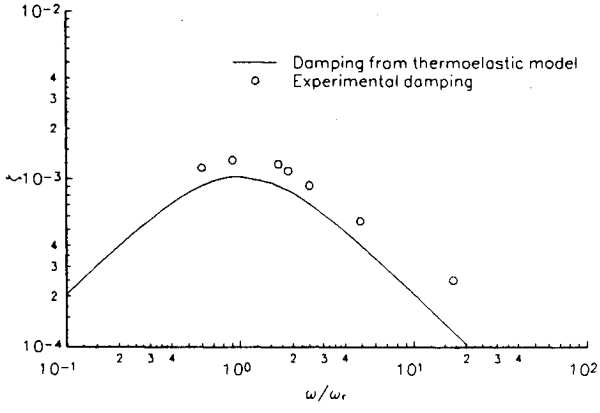

Fig. 3 Theoretical and experimental damping ratios plotted vs nondimensional frequency.

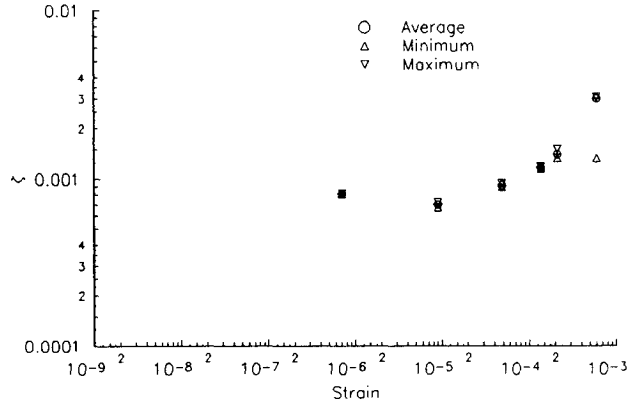

Fig. 4 Damping in first mode of 0.5-m aluminum bar in vacuum, f = 58.1 Hz.

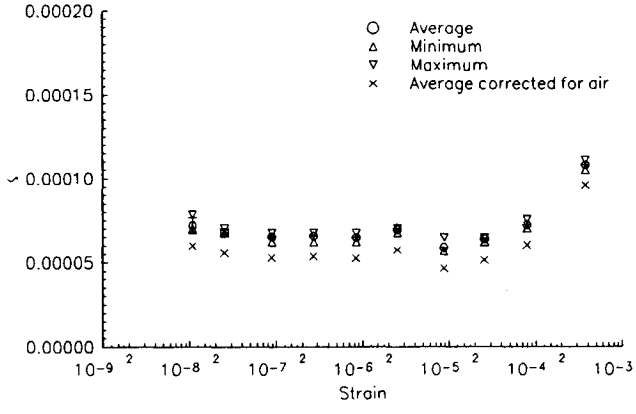

Fig. 5 Damping in first mode of 0.9-m aluminum tube in air, f = 185.1.

Tests over the range of larger strain (1–1000 $\mu\varepsilon$), which were performed in vacuum, show an increase in damping with strain amplitude. As shown in Fig. 4, for the test of the first mode of the 0.5-m aluminum bar, the damping increases with increasing amplitude. This effect, which is evident at strains above 100 $\mu\varepsilon$, can be correlated with a model developed by Boser for damping at large strains.[13] This model assumes that damping at large strain levels is dominated by friction in the crystal lattice due to the motion of dislocations that occurs during plastic deformation. The friction is related to the amount and concentration of impurities in the material, the lattice structure of the material, and the strain levels in the structure. Applying this model to the data obtained from the damping in the first mode of the 0.5-m aluminum bar to obtain a dislocation density yields a density of 1.74×10^6 cm^{-2}. This number is within the range of 10^5–10^7, which is typical of metals.[20]

Results from the tests of the aluminum tubes, summarized in Table 1, show lower average values of damping than those of the bars. At small strain levels, from 10 nε to 100 $\mu\varepsilon$, damping is largely independent of the maximum strain amplitude in the specimen. This strain independence is illustrated in Fig. 5 by the results from the tests of the first mode of the 0.9-m aluminum tube. As shown in Fig. 5, for the first mode of the 0.9-m aluminum tube, damping is independent of strain up to a level of 100 $\mu\varepsilon$. Due to the more complicated geometry of the tube, the thermoelastic relaxation of the Zener model is not as prevalent, resulting in significantly lower damping. Results from the first mode of the 0.7-m aluminum tube tested in vacuum over the larger strain level again shows an increase in damping at a strain of 10$\mu\varepsilon$, yielding a dislocation density of 2.94×10^5 cm^{-2} that again lies in the typical range for metals.[20]

In summary, the damping in both the aluminum bars and tubes shows little variation for small strain levels below 10 $\mu\varepsilon$. For the aluminum bars, the experimentally obtained damping compares well with the predictions of the Zener model and is shown to be frequency dependent. The authors are unaware of any models that predict the damping of metallic tubes, but the fact that the damping in the tubes is independent of frequency and an order of magnitude lower than in the aluminum bars implies that the damping in the tubes is not thermoelastic in origin. At larger strain levels, above 10 $\mu\varepsilon$, both the tubes and the bars seem to show an increase in damping with the maximum strain in the specimen. Keeping in mind the fact that the strain varies along the length of the specimen, this increase can be correlated with the model of damping developed by Boser.

Graphite/Epoxy

Although aluminum is a common material with well-documented damping, its high coefficient of thermal expansion rules out its use as the primary structure of a precision spacecraft. AS4/3501-6 graphite/epoxy, a composite material

Table 2 Material damping test results for graphite/epoxy

Type	Length, m	Freqs. tested, Hz	Strain independent range	Average measured damping ratio	Corrected measured damping ratio	Predicted damping ratio
Gr/Ep	0.9	30.9	3.63 nε– 78.9 με	0.39×10^{-3}	0.29×10^{-3}	0.19×10^{-3}
$[0]_{24}$/bar		83.5	0.863 nε– 41.6 με	0.39×10^{-3}	0.34×10^{-3}	0.19×10^{-3}
Gr/Ep	0.7	56.9	2.46 nε–238 με	0.33×10^{-3}	0.26×10^{-3}	0.19×10^{-3}
$[0]_{24}$/bar		156.9	1.02 nε– 83.8 με	0.38×10^{-3}	0.30×10^{-3}	0.19×10^{-3}
Gr/Ep	0.9	33.2	40.3 nε– 3.63 με	0.78×10^{-3}	0.62×10^{-3}	0.84×10^{-3}
$[\pm 15]_{6s}$/bar		90.8	0.587 nε– 4.20 με	1.17×10^{-3}	0.70×10^{-3}	0.84×10^{-3}
		287.5	3.08 nε–162 με	0.72×10^{-3}	1.11×10^{-3}	0.84×10^{-3}
Gr/Ep	0.7	53.1	1.96 nε– 5.76 με	0.71×10^{-3}	0.63×10^{-3}	0.84×10^{-3}
$[\pm 15]_{6s}$/bar		145.0	0.899 nε–148 με	0.80×10^{-3}	0.75×10^{-3}	0.84×10^{-3}
Gr/Ep	0.9	275.0	4.20 nε– 1.94 με	2.96×10^{-3}	2.93×10^{-3}	——
$[\pm 15]_{3s}$/bar						
Gr/Ep	0.68	503.0	3.76 nε– 9.58 με	1.30×10^{-3}	1.28×10^{-3}	——

commonly used in the aerospace industry, is more typical of materials to be used in the construction of space-based astronomical structures and was the second material studied.[2] Three different types of specimens were constructed from graphite/epoxy, as shown in Table 2. To test the graphite/epoxy material in a layup that might be used in astronomical devices, one set of the 0.9-m and 0.7-m long rectangular bars was constructed with a $[\pm 15]_{6s}$ layup that gave an effectively zero coefficient of thermal expansion. Similarly, the tubes 0.9 m and 0.68 m long were constructed with a $[\pm 15]_{3s}$ layup. To find the effect of layup on damping the second set of bars, 0.9 m and 0.7 m long, were constructed with a $[0]_{24}$, or uniply layup. The graphite/epoxy bars and tube were built with the same cross section as the aluminum bars and tubes.

Results from the tests of the rectangular bars with the $[0]_{24}$ layup are summarized in Table 2. A total of four modes of the two bars were tested over the small strain range in air. For all four modes, the damping is independent of strain amplitude. This behavior is illustrated in Fig. 6 in the plot of damping vs strain for the second mode of the 0.9-m long uniply bar.

The results from the tests of the uniply bars can be compared with the model of damping of uniply structures developed by Hashin[18] and Adams and Bacon.[14] This model assumes that damping of uniply laminates is independent of amplitude. Using the properties of the AS4/3501-6 material,[21] these models produce an estimated value for ζ of 0.19×10^{-3}. This value, listed in Table 2, compares well with the experimental results, slightly underpredicting the actual damping.

Results for the tests of the bars with the $[\pm 15]_{6s}$ layup show similar behavior. A total of five modes of the two bars were tested over the small strain range in air. These results are summarized in Table 2. All five modes showed little variation in damping with amplitude. This behavior is illustrated in Fig. 7, which shows a plot of damping vs strain over a range of strain from 0.899 nε to 148 με for the second mode of the 0.7 m Gr/Ep beam with the $[\pm 15]_{6s}$ layup. When combined with the results from tests conducted in air at higher strains, the results show little variation in strain, over a range of strain from 1 to 1000 με.

These damping ratios can be compared with theory developed by Ni and Adams[15] for laminates with symmetric layups. This model, which predicts that damping depends only on the material and geometric properties, gives an analytical value of ζ of 0.84×10^{-3}. As summarized in Table 2, this value compares well with the experimental results, slightly overpredicting the damping for most cases.

A total of two modes of the graphite/epoxy tubes were tested in air and one in vacuum. Results from the tests of the graphite/epoxy tubes in air are summarized in Table 2. Damping shows little variation with amplitude in the small strain range as illustrated in Fig. 8 in the plot of damping vs strain in the first mode of the 0.7-m-long tube. No attempt was made to correlate the experimentally obtained damping in the tubes because of limitations of time, but research has been performed in the past to develop analytical modes for the damping of laminated tubes.[22,23]

Unlike the aluminum specimens, the damping of the graphite/epoxy tubes is generally higher than that of the bar specimens with a similar layup. It is probable that in the graphite/epoxy tubes and bars, a similar loss mechanism dominates the damping; whereas, in the metal specimens, different mechanisms dominate the damping in the tubes and bars.

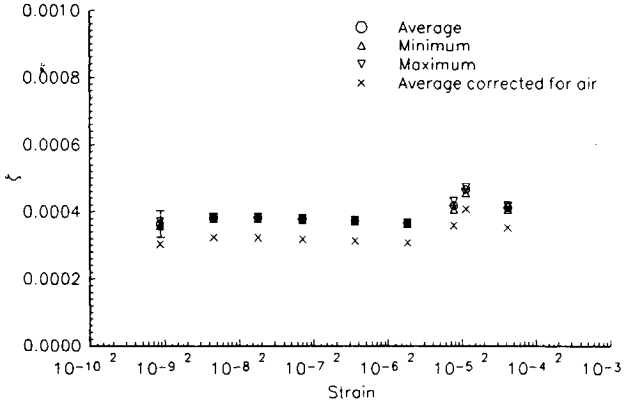

Fig. 6 Damping in second mode of 0.9-m uniply bar in air, f = 83.5 Hz.

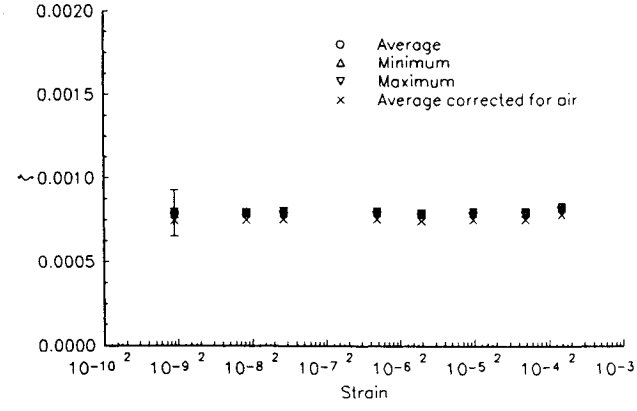

Fig. 7 Damping in second mode of 0.7-m 0 CTE graphite/epoxy bar in air, f = 145.0 Hz.

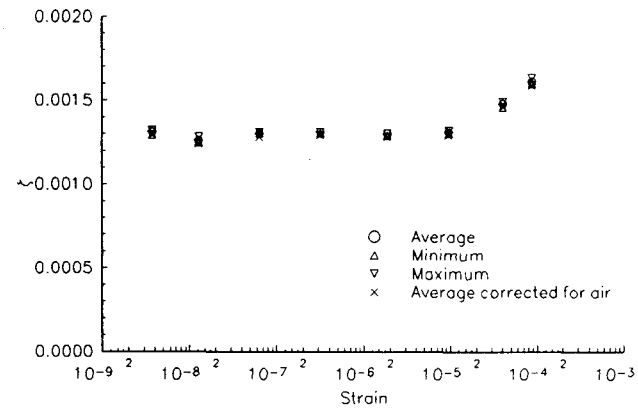

Fig. 8 Damping in the first mode of the 0.7-m [±15]3s graphite/epoxy tube in air, f = 503.0 Hz.

Structural Damping Results

Having established damping over a broad strain range for structural materials, it was desired to investigate the damping in a jointed, built-up structure. To obtain values of structural damping, tests were performed on a model of an interferometric truss, part of a controlled structures testbed developed at Massachusetts Institute of Technology in the Space Engineering Research Center. The essential form of the testbed was a tetrahedral truss, 3.5 m on a side, as shown in Fig. 9. The six legs of the truss were nominally identical, consisting of 14 bays of truss, each 0.25 m long, as shown in Fig. 10. Because of the geometry of the truss layup, two different strut lengths were required: 0.25 m and 0.16 m. Each strut had an outer diameter of 9.5 mm or ⅜ in. and a wall thickness of 1.5 mm. Each node had a 30-mm diameter and had 18 10/32 threaded holes. Both the nodes and the struts were constructed of 6061-T6 aluminum. To connect the nodes to the struts, B nuts were added to the ⅜-24 threaded ends of the struts. The B nuts were hollow caps with female ⅜-24 threads and clearance holes in the ends for 10/32 bolts. To set a strut into a bay, a steel Allen Cap bolt was screwed into a node after having been inserted through the clearance hole in a B nut. As shown in Fig. 10, the cap bolt was secured to the node with two steel nuts and "Loctite." After repeating this on an opposing node, the strut was inserted between the nodes and the two B nuts were screwed to the ends of the strut.

Due to the symmetric geometry of the tetrahedral truss, the lowest global modes were clustered in two frequency ranges. The first bending modes, dominated by the first bending modes of the legs of the truss were clustered between 38 and 58 Hz and the second bending modes, dominated by second bending modes of the legs, were clustered between 94 and 195 Hz. The first bending mode of the longest struts were around 370 Hz.

To sense vibrations, the strut instrumented with the piezoceramic strain sensors was used to replace one of the normal members. The strut was placed in a bay, as shown in Fig. 9, to sense best as many modes as possible. The measured strains were then adjusted using the spatial mode shapes to obtain the maximum strain in the structure. To actuate vibrations, the piezoceramic proof mass actuator or dc motor-driven proof mass actuator was attached to the node next to the instrumented strut, as shown in Fig. 9.

The results from the tests of the testbed are summarized in Table 3 with the average damping ratios, the average damping ratio correct for air effects, the maximum and minimum values, and the strain range over which the damping is independent of strain. All tests were performed in air. Damping ratios were corrected for the effects of air using the same model as for the material damping specimens. Like the material damping test results, the structural damping shows little variation with strain over the small strain range performed

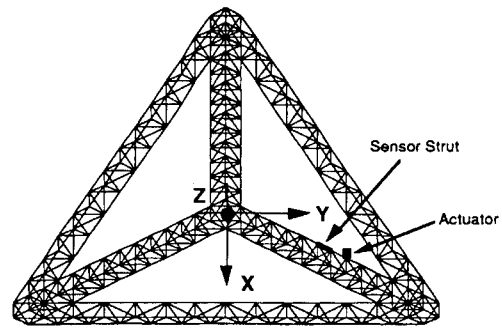

Fig. 9 Instrumentation of interferometer testbed (center vertex of testbed out of plane).

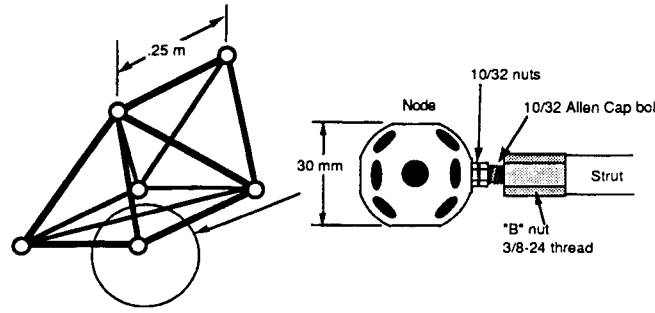

Fig. 10 One bay of tetrahedral truss with a closeup of a joint.

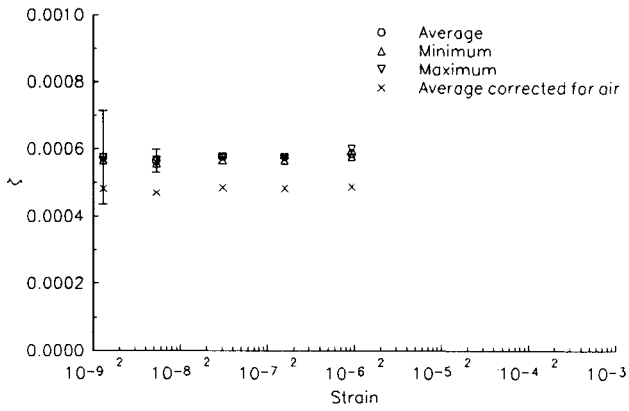

Fig. 11 Damping in mode 1 of testbed, f = 44.1 Hz, small strain range.

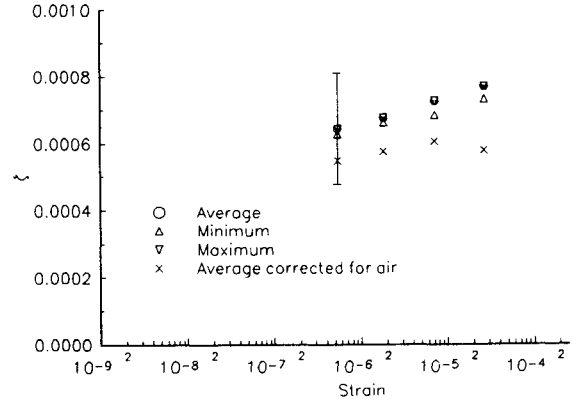

Fig. 12 Damping in mode 1 of testbed, f = 43.9 Hz, large strain range.

Table 3 Structural damping results

Type tested	Mode number	Frequencies tested, Hz	Strain independent range	Average measured damping ratio	Corrected measured damping ratio
Testbed	1	44.1	1.29 nε– 7.01 με	0.58×10^{-3}	0.48×10^{-3}
Testbed	2	40.0	2.02 nε– 6.56 με	0.72×10^{-3}	0.62×10^{-3}
Testbed	3	55.4	2.62 nε–10.9 με	0.65×10^{-3}	0.58×10^{-3}

using the piezoceramic actuator. This behavior is illustrated in Fig. 11 in the plot of damping vs strain obtained from the tests of the mode of the testbed at 44.1 Hz. At larger strain levels, as shown in Fig. 12, using the proof mass actuator for the same mode, the corrected damping ratio also shows little dependence on amplitude. In addition, the mass of the dc motor causes the frequency to decrease from 44.1 to 43.9 Hz.

In summary, the damping in the tetrahedral testbed, like the damping in the material damping specimens, is independent of strain, at least below a certain level, roughly 1 to 10με. This limit is in the same range as the material damping specimens. At strain levels higher than 10 με, damping shows little dependence on strain.

Conclusions

Several conclusions can be drawn from the results of the experiments presented above, concerning both the material and structural damping tests. Results from both tests performed to characterize the behavior of material and structural damping show that the behavior of damping can be divided into two distinct regions: one region at small strain levels, in which the damping is independent of strain and constant down to 1 nε and a second region of large strain levels in which damping increases with peak strain. The bounds on these strain regions and the rate at which damping increases with peak strain, depends on both the material and geometry of the test specimen.

Damping of the aluminum bars and tubes shows little variation with strain level in the small strain region, from 1 nε to about 10 με. The asymptotic lower limit on damping for small strain can be predicted for transverse vibration of the aluminum bars with the thermoelastic model developed by Zener.[4] For transverse vibration of the aluminum tubes, the damping is more than an order of magnitude lower and cannot be correlated with a thermoelastic model. This implies that the damping of the aluminum tubes has a different origin than that of the bars. At larger strain levels, about 100 με, the damping of both the bars and tubes can be modeled using the dislocation model developed by Boser.[13] This model relates the dependence of damping on strain to the dislocation density and lattice properties of metals.

The results from the material damping tests of the graphite/epoxy bars and tubes show that the damping of graphite/epoxy laminates also has an asymptotic lower limit in the small strain region, below 10 με. For laminates with uniply layups and simple, rectangular geometries, this limit can be predicted with models developed by Hashin,[18] and Adams and Bacon.[14] These models relate the damping of a uniply laminate to the properties of the matrix. For more complicated cross-ply laminates, this limit can be predicted with a model developed by Ni and Adams.[15] A change in geometry to a cylindrical cross section seems to have only a small effect on damping. This implies that, unlike the aluminum specimens, the same loss mechanism is present in both the graphite/epoxy bars and tubes. This damping shows a weaker dependence on strain than the damping of the aluminum specimens in the large strain region, above 10 με.

Structural damping, measured from the precision interferometer truss, also shows an asymptotic lower limit in the small strain region, measured using the piezoelectric actuator, at least down to 1 nε. The damping ratios obtained at small strains are almost an order of magnitude greated than the damping of the aluminum tube damping specimens or of the air damping. In the large strain region, above at least 10 με, the damping obtained using the proof mass actuator does not seem to depend on strain level. These results imply that the primary source of the damping of the testbed is other than air and material effects and may be attributed to the joints and attachments or other unknown loss mechanisms.

Another conclusion that can be inferred from the test results is that the instrumentation and methods developed for these experiments can be used to measure and actuate strains down to at least 1 nε. Limitations on the techniques used to measure damping are imposed by the limits of the sensors. Lower limits on the resolution of the piezoelectric sensors are due to mechanical and electrical noise and not due to inherent noise of the sensors. Previous work,[12] verified by the results down to 1 nε from this study, show that the piezoelectric sensors are capable of measuring strains down to at least 10 pε with improved amplification and noise isolation techniques.

References

[1]Dobyns, A., "Aerospace '90—Structures," *Aerospace America*, Vol. 28, No. 12, 1990, pp. 14–15.

[2]Morgan, S. H., Nein, M. E., Davis, B. G., Hamilton, E. C., Roberts, D. H., and Traub, W. A., "Concepts for Large Interferometers in Space," *Society for Petroleum Engineers/Optical Society of America Technology for Space Astrophysics Conference: The Next 30 Years*, AIAA Paper 82-1851.

[3]Garba, J. "Survey of the State of the Art of Microdynamic Response of Structures—Preliminary Results," *Jet Propulsion Laboratory, Interoffice Memorandum*, Nov. 30, 1988.

[4]Zener, C., *Elasticity and Anelasticity of Metals*, University of Chicago Press, Chicago, IL, 1948.

[5]Granick, N., and Stern, J. D., "Material Damping of Aluminum by a Resonant Dwell Technique," NASA TN D-2893, Aug. 1965.

[6]Crawley, E. F., Sarver, G. L., and Mohr, D. G., "Experimental Measurements of Passive Material and Structural Damping for Flexible Space Structures," *Acta Astronautica*, Vol. 10, No. 5–6, 1983.

[7]Lesieutre, G. A., "Damping in Unidirectional Graphite/Metal Composites and Material Design Potential," *Proceedings of the American Society of Mechanical Engineers Vibrations Conference*, Boston, MA, Sept. 1987.

[8]Crawley, E. F., and van Schoor, M. C., "Material Damping in Aluminum and Metal Matrix Composites," *Journal of Composite Materials*, Vol. 21, June 1987.

[9]Gibson, R. F., Plunkett, R., "Dynamic Mechanical Behavior of Fiber Reinforced Composites: Measurement and Analysis," *Journal of Composite Materials*, Vol. 10, No. 10, 1976, pp. 325–341.

[10]Bert, C. W., "Material Damping: An Introductory Review of Mathematical Models, Measures, and Experimental Techniques," *Journal of Sound and Vibration*, Vol. 29, Sec. 2, 1973, pp. 129–153.

[11]Braginsky, V. B., Mitrofanov, V. P., and Panov, V. F., *Systems With Small Dissipation*, The University of Chicago Press, Chicago, IL, 1985.

[12]Forward, R. L., "Picostrain Measurements With Piezoelectric Transducers," *Journal of Applied Physics*, Vol. 51, No. 11, 1980, pp. 5601–5603.

[13]Boser, O., "Internal Friction due to Hysteretic Dislocation Motion in Solid Solution Crystals," *Journal of Applied Physics*, Vol. 54, No. 5, 1983, pp. 2338–2342.

[14]Adams, R. D., and Bacon, D. G. C., "The Dynamic Properties of Unidirectional Fibre Reinforced Composites in Flexure and Tor-

sion," *Journal of Composite Materials*, Vol. 7, No. 1, 1973.

[15]Ni, R. G., and Adams, R. D., "The Damping and Dynamic Moduli of Symmetric Laminated Composite Beams—Theoretical and Experimental Results," *Journal of Composite Materials*, Vol. 18, No. 3, 1984, pp. 104–121.

[16]Piezo Systems, *Piezoelectric Motor/Actuator Kit Manual* (company sales literature), Cambridge, MA, 1989.

[17]Ting, J.M., Crawley, E. F., "Characterization of Damping of Materials and Structures at Nanostrain Levels," NASA Space Engineering Center, Massachusetts Institute of Technology, SERC Rept. 1-90, June 1990.

[18]Ashton, J. E., Halpin, J. C., and Petit, P. H., *Primer on Composite Materials: Analysis*, Technomic Publishing Company, Stamford, CT, 1969.

[19]United States Department of Defense, *Military Standardization Handbook: Metallic Materials and Elements for Aerospace Vehicle Structures*, MIL-HDBK-5C, Vol. 1, Sept. 15, 1976.

[20]Ralls, K. M., Courtney, T. H., and Wulff, J., *Introduction to Materials Science and Engineering*, Wiley, New York, 1976.

[21]Roylance, M. E., Houghton, W. W., and Ghiorse, S. R., "The Effect of Epoxide Purity and Thermal History on the Properties of a Tetrafunctional Epoxy Resin," *Proceedings of the 28th National Society for the Advancement of Material and Process Engineering Symposium and Exhibition*, Anaheim, CA, April 12–14, 1983.

[22]Bicos, A., and Springer, G., "Analysis of Free Damped Vibrations of Laminated Composite Plates and Shells," *International Journal of Solids and Structures*, Vol. 25, No. 2, 1989, pp. 129–149.

[23]Alam, N., and Asnani, N. T., "Vibration and Damping Analysis of Fibre Reinforced Composite Material Shell," *Journal of Composite Materials*, Vol. 21, No. 4, 1987, pp. 348–361.